Low-Temperature Growth of Graphene by Chemical Vapor Deposition Using Solid and Liquid Carbon Sources

Zhancheng Li, Ping Wu, Chenxi Wang, Xiaodong Fan, Wenhua Zhang, Xiaofang Zhai, Changgan Zeng,* Zhenyu Li,* Jinlong Yang, and Jianguo Hou

Hefei National Laboratory for Physical Sciences at Microscale and Department of Physics, University of Science and Technology of China, Hefei, Anhui 230026, China

ABSTRACT Graphene has attracted a lot of research interest owing to its exotic properties and a wide spectrum of potential applications. Chemical vapor deposition (CVD) from gaseous hydrocarbon sources has shown great promises for large-scale graphene growth. However, high growth temperature, typically 1000 °C, is required for such growth. Here we demonstrate a revised CVD route to grow graphene on Cu foils at low temperature, adopting solid and liquid hydrocarbon feedstocks. For solid PMMA and polystyrene precursors, centimeter-scale monolayer graphene films are synthesized at a growth temperature down to 400 °C. When benzene is used as the hydrocarbon source, monolayer graphene flakes with excellent quality are achieved at a growth temperature as low as 300 °C. The successful low-temperature growth can be qualitatively understood from the first principles calculations. Our work might pave a way to an undemanding route for economical and convenient graphene growth.

KEYWORDS: graphene · low temperature growth · chemical vapor deposition · solid carbon sources · liquid carbon sources

Graphene, a monolayer of carbon atoms arranged in hexagonal lattices, has been the focus of both fundamental and applied scientific researches.[1−3] Exceptional physical properties, including integer[4,5] and fractional[6,7] quantum Hall effects have been demonstrated. Graphene also shows a wide range of promising applications such as in transistors[8] and transparent electrodes.[9,10] However, graphene produced by the initial exfoliation method is limited by the small size and low yield.[11] Many efforts have been devoted to developing diverse approaches recently, aiming for large-area synthesis of high-quality graphene films.[1,2] Among them, chemical vapor deposition (CVD) from gaseous carbon sources, mainly methane[9,12,13] on catalytic metal substrates (such as Ni[9,12] and Cu[13]) has already shown great promise. CVD growth on Cu foils has attracted particular attention, since it can grow wafer-scale graphene films with uniform single-layer thickness,[13,14] which is attributed to the low solubility of carbon in Cu crystals.

However, the current CVD route requires high growth temperature, typically 1000 °C.[13−17] A low-temperature growth technique is highly desirable, since it is more convenient, economical, environment-friendly, and feasible for industrial application. Very recently, graphene growth was demonstrated by coating polymethylmethacrylate (PMMA) or other solid carbon sources on Cu foils and subsequently annealing above 800 °C.[18] Nevertheless, graphene growth at lower temperature still remains a challenge.

In this Article, a facile and versatile method to grow graphene is developed based on the CVD growth route on Cu foils using solid and liquid carbon sources, which are of low cost and easily accessible. This method features a much lower growth temperature than previously reported.[13−17] For solid PMMA and polystyrene precursors, we acquire centimeter-scale monolayer graphene with excellent quality when the growth temperature is above 800 °C. Graphene can still be achieved even when the growth temperature is lowered down to 400 °C, though the film quality is a little degraded. When benzene is used as the carbon source, high quality monolayer graphene flakes are achieved at a temperature as low as 300 °C. Possible mechanisms on such a low temperature CVD growth are discussed on the basis of first principles calculations.

RESULTS AND DISCUSSION

For solid sources, the revised CVD growth schematic is depicted in Figure 1. The synthesis of graphene was carried out in a split tube furnace. Differing from the previous CVD growth route using gaseous carbon sources,[13−17] here the solid feedstocks loaded

* Address correspondence to cgzeng@ustc.edu.cn, zyli@ustc.edu.cn.

Received for review March 4, 2011 and accepted March 25, 2011.

Published online March 25, 2011
10.1021/nn200854p

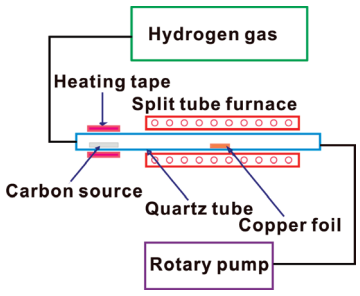

Figure 1. Schematic of the CVD growth from solid carbon sources on Cu foils.

in a small glass container were placed at the gas inlet side of the quartz tube, just outside of the heating zone. Then the Cu foils were annealed to 1000 °C in a 100 sccm H_2 flow for 20 min and cooled down to the desired growth temperature. Subsequently, the solid precursors were heated by a heating tape with the H_2 flow reduced to 50 sccm while maintaining the total pressure between 8 and 15 Torr. The typical growth time was about 45 min. After growth, the furnace was cooled down to room temperature quickly by simply opening the furnace, and the as-grown graphene films were transferred onto a Si substrate with a 300-nm-thick oxide capping layer similar to the method adopted in ref 19.

For the PMMA derived graphene grown at 1000 °C, macroscopic uniformity is achieved, as evidenced from the photograph shown in Figure 2a. Its Raman spectrum (Figure 2b) shows typical characteristics of monolayer graphene: The 2D band centered at ~2682 cm^{-1} is symmetric and can be well fitted by a single Lorentzian peak,[20,21] as shown in the dashed-line box in Figure 2b. The full width at half-maximum (fwhm) of the 2D band is ~37 cm^{-1}, and the intensity ratio of G band to 2D band (I_G/I_{2D}) is ~0.5. Both are similar to the values of methane-derived monolayer graphene grown by CVD on Cu substrate.[13] D band (~1350 cm^{-1}), a measure of defects in the graphene,[22] is absent in the Raman spectrum, demonstrating the high quality of the PMMA derived graphene films. To evaluate the uniformity of the graphene films in large scale, Raman mapping of the fwhm over a 76 × 76 μm^2 area was performed (Figure S1 in the Supporting Information), and the fwhm in most of the investigated area (87%) is below 40 cm^{-1}. We note that the fwhm of bilayer or multilayer graphene grown on Cu foils by CVD is much broader (≥45 cm^{-1}).[15] This indicates the high uniformity of the PMMA-derived monolayer graphene films. The distribution of the fwhm is likely associated with the inhomogeneous external charge doping from the SiO_2/Si substrate.[23−25]

The PMMA derived graphene films were also transferred onto quartz substrates to perform optical transmittance measurement. As depicted in Figure 2c, the transmittance of the graphene film at 550 nm is 97.2%, which agrees well with the value reported for monolayer graphene (97.1%) compared to that of bilayer graphene (94.3%),[18] further confirming the monolayer thickness of the graphene films. Routine scanning electron microscopy (SEM) characterization was also conducted. Figure 2d is an SEM image of the graphene grown at 1000 °C. Graphene wrinkles are clearly resolved, as well as a very few small dark islands on the films. Overall, CVD growth using a PMMA source at 1000 °C obtains superior uniform monolayer graphene.

We then further explored the growth of PMMA-derived graphene at reduced temperatures. At a growth temperature of 800 °C, high-quality monolayer graphene films are still achieved: Raman spectrum (Figure 2b) only shows a noise-level D band and the optical transmittance at 550 nm (Figure 2c) is 96.7%, indicating predominantly monolayer thickness. The typical SEM image (Figure 2e) shows an increases in size and density of the dark islands as compared to the image of graphene grown at 1000 °C, which may account for the slight decrease in the optical transmittance.

Graphene films can actually be grown when the temperature is below 800 °C, even down to 400 °C. The graphene films grown in the temperature range from 700 down to 400 °C show similar microstructure and quality: For graphene films grown at 700 and 400 °C, the Raman spectra (Figure 2b) show a remarkable background signal superimposed on the D and G peaks. Similar features were also observed for graphene with amorphous residual hydrocarbon structures on top.[26] The microstructure was characterized by SEM, as shown in Figure 2panels f and g. The dark features might be some disordered hydrocarbon structures coalesced from the PMMA decomposed fragments at low temperatures, as indicated by the Raman spectra. The inset of Figure 2f shows a sharp edge of the graphene films on the SiO_2/Si substrate, which confirms the continuity of the graphene films grown at low temperature. It is noted that an elongated rectangular pattern with mutually perpendicular sides is clearly evidenced in the SEM image (Figure 2f). The origin of such a pattern is not fully understood, and could result from the (100) facets of the underneath polycrystalline Cu substrate. The optical transmittances at 550 nm of graphene films grown at 700 and 400 °C (Figure 2c) are above 96.5%, similar to that of graphene grown at 800 °C, suggesting that the monolayer still dominates the graphene films. The high optical transmittance renders the graphene films grown at low-temperature ideal candidates for applications in transparent electronics.[9,10]

Another solid carbon source, polystyrene, was also used to synthesize graphene. Polystyrene contains a different molecular formula and structure from PMMA. Using the same procedure for graphene growth from PMMA, we achieved graphene films with similar quality to that of PMMA derived graphene films when the

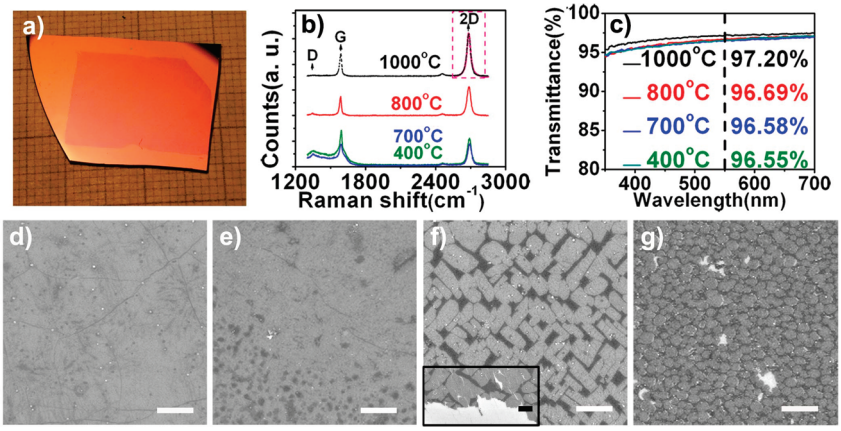

Figure 2. PMMA derived graphene. (a) Photograph of graphene grown at 1000 °C and transferred to the SiO_2/Si substrate. (b) Raman spectra of graphene grown at 1000, 800, 700, and 400 °C, respectively. (c) Optical transmittance spectra of graphene grown at 1000, 800, 700, and 400, respectively. The transmittances of light at 550 nm for different growth temperatures are also indicated in panel c. (d−g) Typical SEM images of graphene grown at 1000, 800, 700, and 400 °C, respectively. The inset of panel f is an SEM image showing the sharp edge of graphene on the SiO_2/Si substrate. The scale bars are 2 μm (d−g, inset of f).

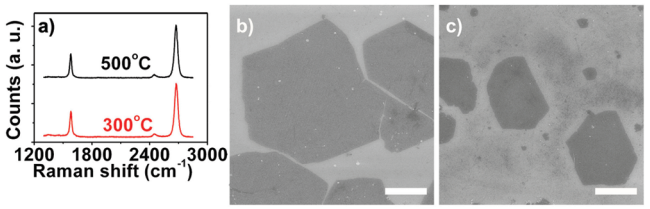

Figure 3. Benzene derived graphene. (a) Raman spectra of graphene grown at 500 and 300 °C, respectively. (b and c) SEM images of graphene grown at 500 and 300 °C, respectively. Scale bars are 2 μm (b and c).

growth temperature is close (see Figure S2 in the Supporting Information). The successful growth of graphene from polystyrene further illustrates the versatility of our low-temperature CVD growth method from solid precursors.

For comparison, we attempted to grow graphene also from a gaseous source (methane) at various temperatures. No graphene can be formed when the growth temperature is lowered to 600 °C (see Figure S3 in the Supporting Information for more details). Therefore, the CVD growth route using solid carbon sources is superior than using gaseous ones at low temperatures. This advantage renders it a simpler and more convenient choice for industrial application.

It is noted that the solid precursors we used have large and complex molecular structures. The graphene synthesis from these precursors involves complicated chemical reactions and processes. At low growth temperatures, decomposition of these large molecules may not be completed, and disordered hydrocarbon structures would therefore develop on the graphene films and degrade the film quality. Further effort is required to search for optimal solid precursors for high-quality graphene growth at low temperature. On the other hand, benzene, a ring-structured molecule, resembles the basic unit of graphene. In contrast to the large molecules such as PMMA or polystyrene, benzene molecules just need to dehydrogenate and connect to each other to form the graphene structure. It might be easier to grow high-quality graphene using benzene precursor at low temperature.

In light of this conjecture, we used a liquid benzene source to grow graphene at low temperature, adopting a similar procedure for CVD growth from solid sources: After the pretreatment of Cu foils at 1000 °C in a 100 sccm H_2 flow for 20 min, liquid benzene loaded in a small glass container was placed in the tube, at the same position as for solid sources. Then the furnace was heated to the desired growth temperature while the benzene source was kept at room temperature. The growth time is usually between 15 and 30 min, with a 50 sccm H_2 flow, while the total pressure was maintained between 8 and 15 Torr. At last, the synthesized graphene was transferred to the SiO_2/Si substrates.

For a growth temperature of 500 °C, the SEM image as shown in Figure 3b clearly reveals the formation of large graphene flakes. Raman spectrum on the flakes (Figure 3a) shows the typical feature of monolayer graphene (fwhm of 2D peak is 37.4 cm^{-1}), and high quality is evidenced by the absence of D band. When the growth temperature was reduced to as low as 300 °C, it is amazing to see that uniform monolayer graphene flakes can still be achieved from the Raman (fwhm of 2D peak is 38 cm^{-1}) and SEM measurements (Figure 3 panels a and c),

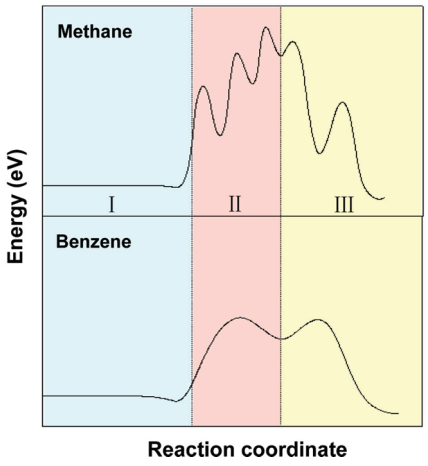

Figure 4. Schematic energy profiles of graphene growth with methane and benzene as carbon sources.

although the flake size is a little smaller than that grown at 500 °C. The D band in the Raman spectrum is at the noise level, confirming the high quality even at a low growth temperature of 300 °C. The flakes usually have well-defined corners which are predominantly 120°. This differs from the commonly seen starlike shape of graphene flakes grown by low-pressure CVD from methane.[13,17] It is noted that graphene grains with corners of 120° have been reported for ultralow-pressure CVD growth at 1035 °C,[27] and ambient CVD growth at 1050 °C[28] from a methane precursor. The mechanism for this kind of shape formation is unknown and needs further exploration. We also tried lower growth temperature of 200 °C, but no graphene is formed as can be seen from the Raman and SEM characterization. This might be due to insufficient energy for hydrogen detachment and further graphene formation at such a low temperature. Thus the synthesis of monolayer graphene with excellent quality from benzene is realized successfully at a surprising low temperature of 300 °C.

To understand the mechanism of low-temperature graphene growth by solid and liquid carbon sources, we divide the CVD growth of graphene into three stages. At stage I, precursor molecules collide to the surface, and they can either adsorb on it, scatter back to the gas phase, or directly proceed to the next stage reaction. Then, at stage II, the carbon source molecules dehydrogenate or partially dehydrogenate, forming active surface species. Finally, these active species coalesce, nucleate, and grow to graphene. Here, we use methane and benzene as two examples to compare differences between gas and liquid/solid carbon precursors at these three stages.

First, we compare the adsorption energies of methane and benzene on a Cu (111) surface. Both are very small, while the former is almost zero (0.02 eV) and the latter is relatively large (0.09 eV). Larger adsorption energy means that trapping-mediated processes are more relevant. Typically, a trapping-mediated reaction has a lower activation energy compared to that of a direct process.[29] Therefore, at stage I, benzene has a slight tendency for lower growth temperature.

Dehydrogenation at stage II is an important process for graphene growth on a Cu surface. The calculated activation energy of benzene dehydrogenation on Cu (111) is 1.47 eV, which is lower than that of methane (1.77 eV). More importantly, smaller gas phase molecules usually need to lose more than one hydrogen atom before they become active and ready for coalescence and nucleation. During the step-by-step dehydrogenation reactions, the energy becomes higher and higher,[30] which requires a high temperature to populate high energy intermediates. Thus, the overall effective dehydrogenation barrier of methane is much higher than benzene (Figure 4).

The third stage of graphene growth involves coalescence of the active species on the Cu surface generated by dehydrogenation or partial dehydrogenation, their nucleation, and finally the formation of graphene. This stage is the most complicated one. However, many relevant elementary reactions have been studied previously, such as incorporation of atomic carbon[31] and combination of CH groups.[30] These elementary processes generally have an activation energy between 1.0 and 2.0 eV. Although this does not directly lead to an activation behavior difference between benzene and methane, we notice that benzene already has a six-numbered carbon ring structure, while several high energy intermediates may exist for methane to form large hydrocarbon structure. For example, according to our calculation, on a Cu (111) surface, a two-C_3H_3 group is 3.66 eV higher than benzene. Methane thus should have a larger nucleation barrier compared to benzene. Finally, combining these differences at the three stages, we can understand qualitatively the much lower temperature required to grow graphene from benzene than from methane.

CONCLUSION

We have demonstrated a simple CVD route to grow high-quality graphene at low temperature, adopting solid and liquid carbon feedstocks. For solid PMMA and polystyrene precursors, monolayer graphene films are synthesized in large scale when the growth temperature is above 800 °C. Graphene films can still be achieved even when the growth temperature is lowered down to 400 °C, at the expense of a little downgrade in film quality. When benzene is used as the carbon source, monolayer graphene flakes with excellent quality are achieved at a temperature as low as 300 °C. Possible mechanisms on such a low temperature CVD growth are discussed based on first principles

calculations. The proposed low-temperature growth method adopting solid/liquid carbon sources might pave a way to an undemanding route for economical and convenient graphene growth.

METHODS

Graphene Growth from Solid Carbon Sources. At first, the solid feedstocks, loaded in a small glass container with an aperture of 1 cm, were placed at the gas inlet side of the quartz tube, just outside of the heating zone. The 25 μm-thick Cu foils (Alfa Aesar, item No. 13382) were then annealed to 1000 °C in a 100 sccm H_2 flow for 20 min and cooled down to the desired growth temperature (1000, 800, 700, 500, and 400 °C, respectively). The solid precursors were subsequently heated by a heating tape wrapped around the quartz tube (the heating temperature is about 140 °C for PMMA and 260 °C for polystyrene) with the H_2 flow reduced to 50 sccm while maintaining the total pressure between 8 and 15 Torr. The typical growth time was about 45 min. After growth, the furnace was opened for fast cooling. The as-grown graphene films were eventually transferred onto Si substrates with a 300-nm-thick oxide capping layer.

Graphene Growth from Benzene Source. Cu foil was initially cleaned at 1000 °C in a 100 sccm H_2 flow for 20 min and then cooled to room temperature. After the Cu pretreatment, liquid benzene loaded in a small glass container (same size as for solid precursors) was placed in the tube, just outside of the heating zone. To reduce the evaporation rate of benzene, the aperture of the container was wrapped with aluminum foil, and 2−3 pinholes with diameter of only 0.5 mm were pricked in the foil. Then the furnace was heated to the desired growth temperature (500, 300, and 200 °C, respectively) while the benzene source was kept at room temperature. The growth time was usually between 15 and 30 min, with a 50 sccm H_2 flow during growth while the total pressure was maintained between 8 and 15 Torr. At last, the synthesized graphene was transferred to the SiO_2/Si substrates.

Sample Characterization. Raman spectroscopy (French JY LABRAM-HR) with a laser excitation wavelength of 514.5 nm (the beam size is 2 μm in diameter) was used to characterize the thickness, quality, and uniformity of the grown graphene films at room temperature. Optical transmittance spectra were measured using a UV−vis−NIR spectrophotometers (Shimadzu DUV-3700). The morphology of graphene films was characterized using a field emission SEM (FEI Sirion 200) operated at 5 kV.

First Principles Calculations. Density functional theory implemented in the VASP package[32] with PW91 exchange-correlation functional[33] is adopted. Single electron states are represented by plane waves with a cutoff energy of 400 eV. A four-layer slab model is used to describe the Cu(111) surfaces, in which the bottom layer is fixed to its optimized bulk geometry. Repeated slabs were separated by more than 10 Å to avoid interactions between neighboring slabs. P(3×3) and p(4×5) unit cells are used to model hydrocarbon absorption.

Acknowledgment. We appreciate support from the Fundamental Research Funds for the Central Universities (Grant No. WK2340000011), NSFC (Grants Nos. 10974188, 91021018, 20933006, and 11034006), ``One-hundred-person Project'' of CAS, NKBRPC (Grant No. 2009CB929502), NCET, and CPSFFP (Grant No. 20100470837).

Supporting Information Available: Additional Raman and SEM characterizations of graphene grown from PMMA, polystyrene, and methane. This material is available free of charge *via* the Internet at http://pubs.acs.org.

REFERENCES AND NOTES

1. Geim, A. K. Graphene: Status and Prospects. *Science* **2009,** *324*, 1530–1534.
2. Zhu, Y. W.; Murali, S.; Cai, W. W.; Li, X. S.; Suk, J. W.; Potts, J. R.; Ruoff, R. S. Graphene and Graphene Oxide: Synthesis, Properties, and Applications. *Adv. Mater.* **2010,** *22*, 3906–3924.
3. Dresselhaus, M. S.; Araujo, P. T. Perspectives on the 2010 Nobel Prize in Physics for Graphene. *ACS Nano* **2010,** *4*, 6297–6302.
4. Novoselov, K. S.; Geim, A. K.; Morozov, S. V.; Jiang, D.; Katsnelson, M. I.; Grigorieva, I. V.; Dubonos, S. V.; Firsov, A. A. Two-Dimensional Gas of Massless Dirac Fermions in Graphene. *Nature* **2005,** *438*, 197–200.
5. Zhang, Y.; Tan, Y. W.; Stormer, H. L.; Kim, P. Experimental Observation of the Quantum Hall Effect and Berry's Phase in Graphene. *Nature* **2005,** *438*, 201–204.
6. Du, X.; Skachko, I.; Duerr, F.; Luican, A.; Andrei, E. Y. Fractional Quantum Hall Effect and Insulating Phase of Dirac Electrons in Graphene. *Nature* **2009,** *462*, 192–195.
7. Bolotin, K. I.; Ghahari, F.; Shulman, M. D.; Stormer, H. L.; Kim, P. Observation of the Fractional Quantum Hall Effect in Graphene. *Nature* **2009,** *462*, 196–199.
8. Schwierz, F. Graphene Transistors. *Nat. Nanotechnol.* **2010,** *5*, 487–496.
9. Kim, K. S.; Zhao, Y.; Jang, H.; Lee, S. Y.; Kim, J. M.; Kim, K. S.; Ahn, J. H.; Kim, P.; Choi, J. Y.; Hong, B. H. Large-Scale Pattern Growth of Graphene Films for Stretchable Transparent Electrodes. *Nature* **2009,** *457*, 706–710.
10. Becerril, H. A.; Mao, J.; Liu, Z.; Stoltenberg, R. M.; Bao, Z.; Chen, Y. Evaluation of Solution-Processed Reduced Graphene Oxide Films as Transparent Conductors. *ACS Nano* **2008,** *2*, 463–470.
11. Novoselov, K. S.; Geim, A. K.; Morozov, S. V.; Jiang, D.; Zhang, Y.; Dubonos, S. V.; Grigorieva, I. V.; Firsov, A. A. Electric Field Effect in Atomically Thin Carbon Films. *Science* **2004,** *306*, 666–669.
12. Reina, A.; Jia, X. T.; Ho, J.; Nezich, D.; Son, H. B.; Bulovic, V.; Dresselhaus, M. S.; Kong, J. Large Area, Few-Layer Graphene Films on Arbitrary Substrates by Chemical Vapor Deposition. *Nano Lett.* **2009,** *9*, 30–35.
13. Li, X. S.; Cai, W.; An, J.; Kim, S.; Nah, J.; Yang, D.; Piner, R.; Velamakanni, A.; Jung, I.; Tutuc, E.; *et al.* Large-Area Synthesis of High-Quality and Uniform Graphene Films on Copper Foils. *Science* **2009,** *324*, 1312–1314.
14. Bae, S.; Kim, H.; Lee, Y.; Xu, X.; Park, J. S.; Zheng, Y.; Balakrishnan, J.; Lei, T.; Kim, H. R.; Song, Y. I.; *et al.* Roll-to-Roll Production of 30-Inch Graphene Films for Transparent Electrodes. *Nat. Nanotechnol.* **2010,** *5*, 574–578.
15. Lee, S; Lee, K; Zhong, Z. H. Wafer Scale Homogeneous Bilayer Graphene Films by Chemical Vapor Deposition. *Nano Lett.* **2010,** *10*, 4702–4707.
16. Li, X. S.; Cai, W. W.; Colombo, L.; Ruoff, R. S. Evolution of Graphene Growth on Ni and Cu by Carbon Isotope Labeling. *Nano Lett.* **2009,** *9*, 4268–4272.
17. Li, X. S.; Magnuson, C. W.; Venugopal, A.; An, J. H.; Suk, J. W.; Han, B. Y.; Borysiak, M.; Cai, W. W.; Velamakanni, A.; Zhu, Y. W.; *et al.* Graphene Films with Large Domain Size by a Two-Step Chemical Vapor Deposition Process. *Nano Lett.* **2010,** *10*, 4328–4334.
18. Sun, Z. Z.; Yan, Z.; Yao, J.; Beitler, E.; Zhu, Y.; Tour, J. M. Growth of Graphene from Solid Carbon Sources. *Nature* **2010,** *468*, 549.
19. Li, X. S.; Zhu, Y.; Cai, W.; Borysiak, M.; Han, B.; Chen, D.; Piner, R. D.; Colombo, L.; Ruoff, R. S. Transfer of Large-Area Graphene Films for High-Performance Transparent Conductive Electrodes. *Nano Lett.* **2009,** *9*, 4359–4363.
20. Ferrari, A. C.; Meyer, J. C.; Scardaci, V.; Casiraghi, C.; Lazzeri, M.; Mauri, F.; Piscanec, S.; Jiang, D.; Novoselov, K. S.; Roth, S.; *et al.* Raman Spectrum of Graphene and Graphene Layers. *Phys. Rev. Lett.* **2006,** *97*, 187401.

21. Graf, D.; Molitor, F.; Ensslin, K.; Stampfer, C.; Jungen, A.; Hierold, C.; Wirtz, L. Spatially Resolved Raman Spectroscopy of Single- and Few-Layer Graphene. *Nano Lett.* **2007,** *7*, 238–242.
22. Malard, L. M.; Pimenta, M. A.; Dresselhaus, G.; Dresselhaus, M. S. Raman Spectroscopy in Graphene. *Phys. Rep.* **2009,** *473*, 51–87.
23. Berciaud, S. P.; Ryu, S.; Brus, L. E.; Heinz, T. F. Probing the Intrinsic Properties of Exfoliated Graphene: Raman Spectroscopy of Free-Standing Monolayers. *Nano Lett.* **2009,** *9*, 346–352.
24. Casiraghi, C.; Pisana, S.; Novoselov, K. S.; Geim, A. K.; Ferrari, A. C. Raman Fingerprint of Charged Impurities in Graphene. *Appl. Phys. Lett.* **2007,** *91*, 233108.
25. Ni, Z. H.; Yu, T.; Luo, Z. Q.; Wang, Y. Y.; Liu, L.; Wong, C. P.; Miao, J.; Huang, W.; Shen, Z. X. Probing Charged Impurities in Suspended Graphene Using Raman Spectroscopy. *ACS Nano* **2009,** *3*, 569–574.
26. Lin, Y. C.; Jin, C.; Lee, J. C.; Jen, S. F.; Suenaga, K.; Chiu, P. W. Clean Transfer of Graphene for Isolation and Suspension. *ACS Nano* **2011,** *5*, 2362–2368.
27. Li, X.; Magnuson, C. W.; Venugopal, A.; Tromp, R. M.; Hannon, J. B.; Vogel, E. M.; Colombo, L.; Ruoff, R. S. Large-Area Graphene Single Crystals Grown by Low-Pressure Chemical Vapor Deposition of Methane on Copper. *J. Am. Chem. Soc.* **2011,** *133*, 2816–2819.
28. Yu, Q. K.; Jauregui, L. A.; Wu, W.; Colby, R.; Tian, J. F.; Su, Z. H.; Cao, H. L.; Liu, Z. H.; Pandey, D.; Wei, D. G.; *et al.* Single-Crystal Grains and Grain Boundaries in Graphene Grown by Chemical Vapor Deposition. arXiv:1011.4690v1, 2010 (Accessed November 21, 2010).
29. Jachimowski, T. A.; Hagedorn, C. J.; Weinberg, W. H. Direct and Trapping-Mediated Dissociative Chemisorption of Methane on Ir(111). *Surf. Sci.* **1997,** *393*, 126–134.
30. Zhang, W.; Wu, P.; Li, Z.; Yang, J. First-Principles Thermodynamics of Graphene Growth on Cu Surface. arXiv:1101.3851, 2011 (Accessed January 20, 2011).
31. Wu, P.; Zhang, W.; Li, Z.; Yang, J.; Hou, J. G. Communication: Coalescence of Carbon Atoms on Cu (111) Surface: Emergence of a Stable Bridging-Metal Structure Motif. *J. Chem. Phys.* **2010,** *133*, 071101.
32. Kresse, G.; Furthmuller, J. Efficient Iterative Schemes for *ab Initio* Total-Energy Calculations Using a Plane-Wave Basis Set. *Phys. Rev. B* **1996,** *54*, 11169–11186.
33. Perdew, J. P.; Chevary, J. A.; Vosko, S. H.; Jackson, K. A.; Perderson, M. R.; Singh, D. J.; Fiolhais, C. Atoms, Molecules, Solids, and Surfaces: Applications of the Generalized Gradient Approximation for Exchange and Correlation. *Phys. Rev. B* **1992,** *46*, 6671–6687.